AUTOMATED TENSION CONTROL SYSTEM OF TRACK BELT FOR BULLDOZING OPERATION

Tatsuro MURO, Prof. Department of Ocean Engineering
Faculty of Engineering, Ehime University

3 Bunkyo-cho, Matsuyama 790, Japan

SUMMARY

As the flexibility of track belt running on a weak terrain affects the shape of contact pressure distribution, the flexibility is dominant not only over the thrust developed under the track belt but over the amount of slip sinkage at the rear sprocket. Here, the relations between track tension, normal and shear stress distribution, and the amount of static and slip sinkages have been presented for a flexible tracked bulldozer running on a weak silty loam terrain by means of the rigorous simmulation programme. As the results, it is clarified that the effective tractive effort increases monotonously and the amount of total sinkage of rear sprocket decreases remarkably with the increment of track tension. For adjusting the track tension to the optimum flexibility corresponding to the running terrain, an automated tension control system of the track belt should be established by use of some track tension sensor or rut depth sensor.

Key words : *track tension, flexible tracked vehicle, effective tractive effort, weak terrain, sinkage*

1. Introduction

The productivity of bulldozer having a flexible track belt running on a weak terrain is considered to vary remarkably with the flexibility of the track belt. It is necessary to control the track belt tension in moderate state at all times, because the tension used to drop down gradually due to the abrasive wear of tread parts of frontidler, pin and bush of link etc.. As there is an optimum flexibility of track belt for a given terrain to maximize the optimum effective tractive effort, the flexibility should be considered as one of the most important factors to obtain the maximum productivity or the maximum efficiency of bulldozer. The shape of distribution of contact pressure depends considerably on the flexibility, so the track tension gives an important effect on the thrust developed under the track belt and the rut depth of bulldozer. Here, several relations between the track tension, the effective tractive effort, and the amount of sinkage of rear sprocket have been analysed for a given bulldozer running on the weak ground of given terrain-track system constants by means of the new developed simmulation programme. Afterwards, several methods to set the control system of the flexibility of track belt are considered by use of some tension sensor or rut depth sensor.

2. Flexibility and track tension

Fig.1 shows the several forces acting on the flexible track belt.

The following condition of equilibrium may be written if the denotations in the figure are followed :

$$F = T_o \tan\delta = T_o \frac{d\, S_{oi}'(X)}{d\, X} \qquad (1)$$

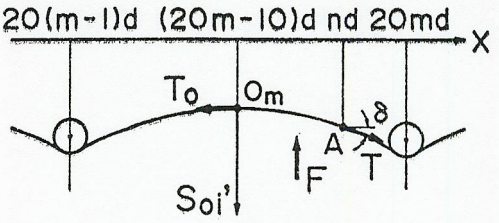

Fig.1 Several forces acting on flexible track belt

where F is the ground reaction between the central point O_m of the adjacent two track rollers and the arbitrary point A, T_o is the tension force acting upon the point O_m, and $S_{oi}'(X)$ is the amount of static sinkage of track belt at the distance X from the contact point of frontidler on the main part of track belt [1].

The ground reaction $F = F(X)$ could be calculated approximately as the integration of normal contact pressure $p_{oi}(X)$ of rigid track belt from the point O_m : $X = (20m-10)d$ to the point A : $X = n\,d$ where m, n is a positive integer and $d = D/N$ is the minute interval of the contact length of track belt D. That is,

$$F(X) = B \int_{(20m-10)d}^{nd} p_{oi}(X)\, dx \qquad (2)$$

$$(20m-20 < n < 20m)$$

where B is the track width.

And T_o is the summation of the initial track tension force H_o and the thrust H_m acting upon the interface of track belt and ground. H_m could be calculated as the integration of shear resistance $\tau(X)$ of ground from the contact point of frontidler on the main part of track belt : $X = 0$ to the point O_m : $X = (20m-10)d$. That is,

$$H_m = B \int_{0}^{(20m-10)d} \tau(X)\, dX \quad . \qquad (3)$$

Therefore, the distribution of static sinkage of the flexible track belt could be calculated from Eqs.(1)(2) and (3) as,

$$S_{oi}'(X) = \frac{1}{H_o + H_m} \int_{(20m-10)d}^{nd} F(X)\, dX + C$$

$$C = S_{oi}\{(20m-10)d\} \qquad (4)$$

where C is the static sinkage of rigid track belt at $X = (20m-10)d$.

Then, the distribution of normal contact pressure $p_{oi}'(X)$ of the flexible track belt could be calculated as

$$p_{oi}'(X) = k\,\{S_{oi}'(X)\}^n \quad . \qquad (5)$$

On the other hand, the total sinkage of frontidler S_{fi}' could be calculated as

$$S_{fi}' = \{S_{oi}'(0) + S_{fs}'\}\cos\theta_{ti}' \qquad (6)$$

S_{fs}' is the slip sinkage [2] given as

$$S_{fs}' = c_0 \sum_{m=1}^{M} \{p_{roi}'(\theta_m)\}^{c1}[(j_m)^{c2} - (j_{m-1})^{c2}]\cos\theta_m$$

$$p_{roi}'(\theta_m) = k\,\{S(\theta_m)\}^n$$

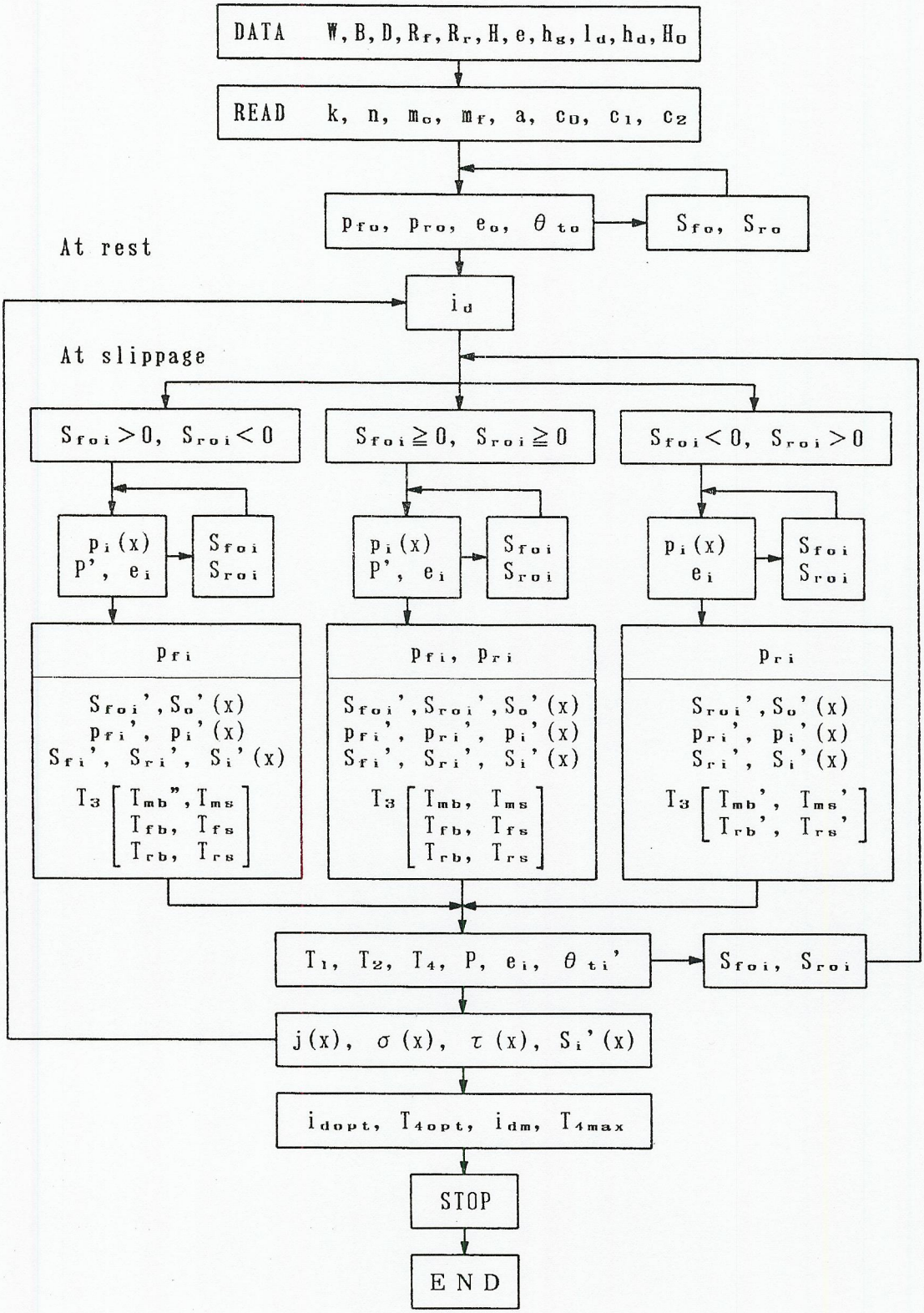

Fig.2 Flow chart

$$S(\theta_m) = \frac{R_f\{\cos(\theta_m+\theta_{ti})-\cos(\theta_f+\theta_{ti})\}}{\cos(\theta_m+\theta_{ti})}$$

$$\theta_m = \theta_f(1-m/M)$$

$$\theta_f = \cos^{-1}(\cos\theta_{ti}' - \frac{S_{fi}'}{R_f}) - \theta_{ti}'$$

$$\theta_{ti}' = \sin^{-1}(\frac{S_{ri}'-S_{fi}'}{D})$$

$$j_m = \frac{R_f}{1-i_d}\int_{\theta m}^{\theta f}\{1-(1-i_d)\cos\theta\}\cos\theta \; d\theta$$

where c_0, c_1 and c_2 are constants, R_f is the radius of frontidler, i_d is slip ratio at driving state and θ_{ti}' is the trim angle of vehicle.

The total sinkage of rear sprocket S_{ri}' could be calculated as

$$S_{ri}' = \{S_{oi}'(D)+S_{rs}'\}\cos\theta_{ti}' \tag{7}$$

S_{rs}' is the slip sinkage given as

$$S_{rs}' = S_{fs}' + c_0\sum_{n=1}^{N}\{p_{oi}'(n\,d)\}^{c1}[(n\,q)^{c2}-\{(n-1)q\}^{c2}]$$

$$p_{oi}'(n\,d) = k\{S_{oi}'(n\,d)\}^n$$

$$q = i_d' D/\{(1-i_d')N\}$$

The contact points among frontidler, each track roller, rear sprocket and main part of flexible track belt should be located on the next straight line.

$$S_i'(X) = S_{fi}' + (S_{ri}'-S_{fi}')\frac{X}{D} \tag{8}$$

Therefore, the final sinkage of flexible track belt $S_i'(n\,d)$ at $X=n\,d$ could be calculated for 7 intervals of track roller as

$$\begin{aligned} S_i'(n\,d) = {} & S_{oi}'(n\,d) + S_i'\{(20m-20)d\} - S_{oi}'\{(20m-20)d\} \\ & + [\{S_i'(20m\,d)-S_{oi}'(20m\,d)\} - [S_i'\{(20m-20)d\} \\ & - S_{oi}'\{(20m-20)d\}]]\cdot\{n\,d-(m-1)\frac{D}{8}\}/\frac{D}{8} \end{aligned} \tag{9}$$

$$d = D/N, \quad 20m-20 < n < 20m$$

$$m = 1, 2, \cdots, 8$$

$$n = 1, 2, \cdots, N\ (160)$$

3. Simmulation programme

Table 1 shows the terrain-track system constants [3] measured for the track model having 5 trapezoidal grousers of 6cm height, 18cm pitch, 2cm contact length and 9cm base which runs on the remolded silty loam terrain of 30% water content and 31kPa Cone Index. Table 2 shows the vehicle dimensions of a given bulldozer having the flexible track belt of the same trapezoidal grousers.

Fig.2 shows the flow chart to calculate the traffic performance of the flexible tracked vehicle running on the weak terrain. First of all, the initial data : W, B, D, R_f, R_r, H, e, h_g, l_d, h_d and H_0 are given. And the terrain-track system constants k, n, m_c, m_f, a, c_0, c_1 and c_2 are read as input data. At rest, the eccentricity e_0 of resultant normal force P acting upon the track belt, the contact pressure p_{fo}, p_{ro} at frontidler and rear sprocket, the trim angle of vehicle θ_{to}

Table 1 Vehicle dimensions

Vehicle Weight	W	117.6 kN
Width of track belt	B	150 cm
Contact length of track belt	D	280 cm
Mean contact pressure	p_m	13.7 kPa
Radius of frontidler	R_f	35 cm
Radius of rear sprocket	R_r	35 cm
Height of grouser	H	6 cm
Grouser pitch	G_p	18 cm
Interval of track roller	R_p	35 cm
Eccentricity of gravity center of vehicle	e	−0.02
Height of gravity center of vehicle	h_g	70 cm
Distance between central axis of vehicle and point acting effective tractive effort	l_d	290 cm
Height of point acting effective tractive effort	h_d	42 cm

Table 2 Terrain-track system constants

Static pressure sinkage test $k = 6.669$ $n = 0.594$
Shear deformation test $m_c = 3.626$ kPa $m_f = 0.356$ $a = 0.148$ 1/cm
Slip sinkage test $c_0 = 0.253$ $c_1 = 0.751$ $c_2 = 0.360$

are repeatedly calculated until the static sinkage S_{fo} , S_{ro} at frontidler and rear sprocket are determined. At slippage state for a given i_d , the contact pressure p_{fi} , p_{ri} and the distribution $p_i(X)$ for an assumed rigid track belt, the modified resultant normal force P' for the force acting upon the frontidler, and the eccentricity e_i are repeated calculated until the static sinkages S_{foi} and S_{roi} are determined. Afterwards, the distributions of static sinkage $S_o'(X)$, S_{foi}' and S_{roi}' , and contact pressure $p_i'(X)$, p_{fi}' and p_{ri}' for the flexible track belt are obtained, and then the distribution of total sinkage $S_i'(X)$ is determined as the summation of $S_o'(X)$ and the slip sinkage calculated from $p_i'(X)$. The thrust T_3 is calculated as the summation of shear resistance which develops on the interface between main part of bottom track belt T_{mb} , T_{ms} , contact part of frontidler T_{fb} , T_{fs} and that of rear sprocket T_{rb} , T_{rs} , and the terrain [2] . Then, the driving force T_1 , the locomotion resistance T_2 , the effective tractive effort T_4 , the resultant normal force P, the eccentricity e_i and the trim angle θ_{ti}' are repeatedly calculated until the static sinkages of the track belt S_{foi} , S_{roi} are determined. There are 3 kinds of process which is divided by the sign of static sinkage of the flexible track belt. Finally, the relations between $T_1, T_4 - i_d$, $S_{fi}', S_{ri}' - i_d$, $\theta_{ti}' - i_d$ and $e_i - i_d$ are determined, and the distributions of amount of slippage $j(X)$, normal stress $\sigma(X)$, shear stress $\tau(X)$ and total sinkage of track belt $S_i'(X)$ are graphically shown by use of microcomputer.

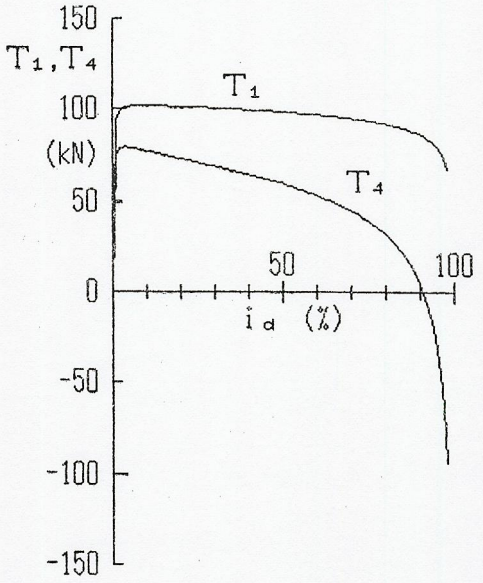

Fig.3 Driving force T_1, effective tractive effort T_4 and slip ratio i_d

4. Analytical results

4.1 Tractive performance

As an example, the tractive performance of the flexible tracked vehicle as shown in Table 2 has been simmulated for the initial track tension force H_o = 9.8kN . Fig.3 shows the relations between T_1, T_4 and i_d at driving state. T_1 decreases gradually with i_d from the maximum value 102.0kN at i_d = 10% and T_4 decreases rapidly with i_d from the maximum one 78.4kN at i_{dm} = 2% due to the increasing locomotion resistance. Fig.4 shows the relations between S_{fi}', S_{ri}' and i_d at driving state. S_{ri}' is always larger than S_{fi}' due to the increasing slip sinkage with slip ratio. Fig.5 shows the relations between e_i, θ_{ti}' and i_d. e_i decreases gradually until the minimum value −0.0694 at i_d = 86% and then in-

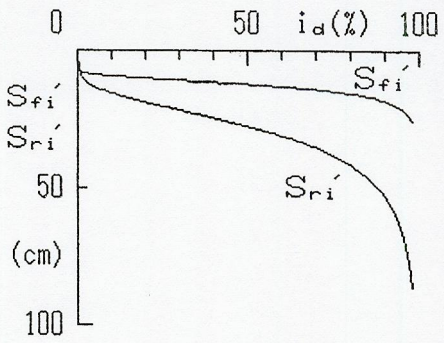

Fig.4 Total sinkages of frontidler and rear sprocket S_{fi}', S_{ri}' and slip ratio i_d

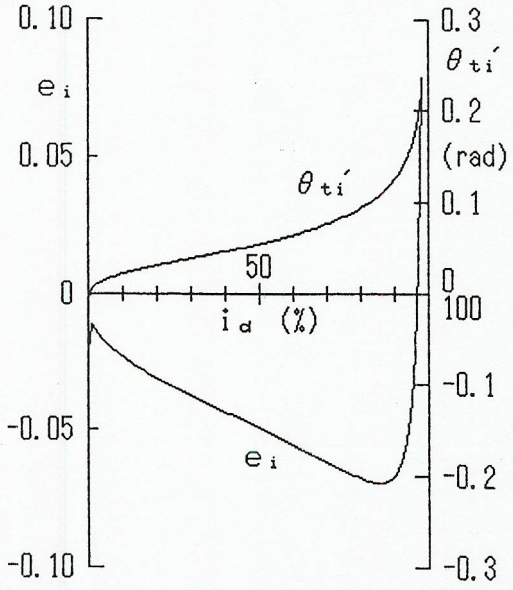

Fig.5 Eccentricity e_i, trim angle θ_{ti}' and slip ratio i_d

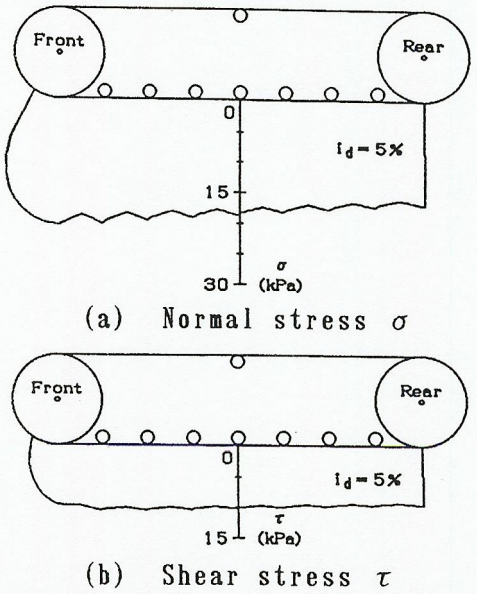

Fig.6 Distribution of contact pressure at driving state

creases rapidly at higher value of slip ratio. θ_{ti}' increases parabolically with the increasing slip sinkage. Fig.6 shows the distributions of normal stress σ and shear stress τ under the bottom track belt for $i_d = 5\%$. It shows some sinusoidal distribution, of which amplitude at front part of track belt is comparatively larger than that at the rear part due to the increasing thrust H_m. The amplitude of deflection of the track belt varies from 0.01cm to 0.52cm.

4.2 Tension control system

The relations between tractive performance and track tension are simmulated for the flexible tracked vehicle. Fig.7 shows the relations between the optimum effective tractive effort T_{4opt} at the optimum slip ratio i_{opt}[3] and the track tension H_o for 3 kinds of eccentricity of the gravity center of the bulldozer. T_{4opt} increases gradually with the increment of H_o. Fig.8 shows the relations between the total sinkage of rear sprocket S_{ri}' and H_o in these cases, respectively. S_{ri}' decreases remarkably at the lower tension with the increment of H_o. Fig.9 shows that the traffic efficiency of power E_t [4] at i_{opt} increases also at the lower tension with the increment of H_o. So, the track tension H_o should be controlled to set at some value as large as possible in these cases, by means of the hydraulic cylinder which is adjusted by some tension sensor or rut depth sensor.

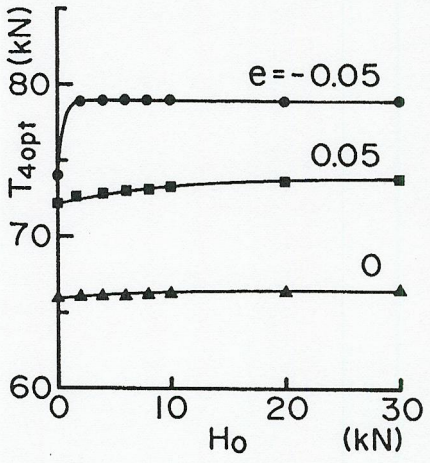

Fig.7 Optimum effective tractive effort T_{4opt} and initial track tension H_o

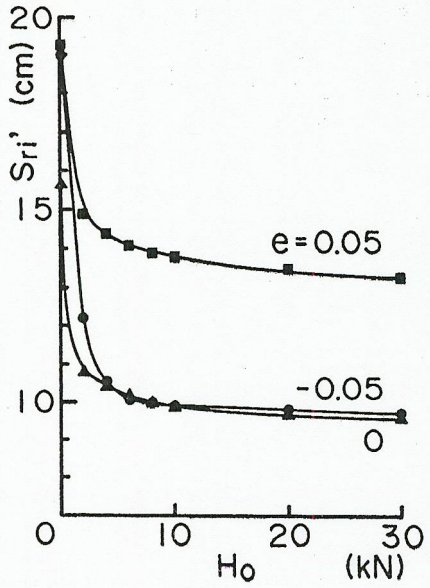

Fig.8 Total sinkage of rear sprocket S_{ri}' and initial track tension H_o

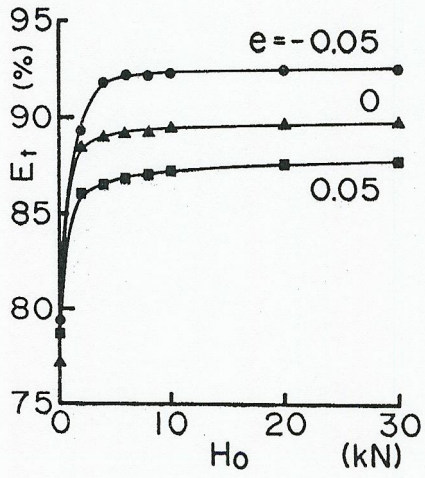

Fig.9 Traffic efficiency of power E_t and initial track tension H_o

5. Conclusion

To establish an optimum operation of a flexible tracked vehicle running on a weak terrain, some tension control system of the track belt should be considered to improve the tractive performance. Here, the rigorous simmulation programme has been developed to analyse the traffic performance of a bulldozer, considering the flexibility of the track belt due to the track tension and the position of track rollers located on a straight line. As the results, the track tension should be controlled to be as large as possible to increase the effective tractive effort and the traffic efficiency of power by means of some track tension sensor or rut depth sensor.

References

1) M. G. Bekker : 1956, Theory of Land Locomotion, The University of Michigan Press, pp.232－288.
2) T. Muro : 1989, Stress and Slippage Distributions under Track Belt Running on a Weak Terrain, Soils and Foundations, Vol.29, No.3, pp.115－126.
3) T. Muro : 1989, Drawbar-pull Control System of a Flexible Tracked Vehicle on Weak Terrain, Proc. of 6th Int. Sympo. on Automation and Robotics in Construction, Construction Industry Institute, pp.260－267.
4) T. Muro : 1988, An Optimum Operation of a Bulldozer Running on a Weak Terrain, Proc. of 5th Int. Sympo. on Robotics in Construction, JSCE, Vol.2, pp.717－726.